Synthesis and Characterization of Novel Functional Inorganic–Organic Hybrid Material with Macromolecule–Metal Complex by Atom Transfer Radical Polymerization

Yaxin Xu, Hongtu Li, Di Wang, Yapeng Li, Yantao Song, Peng Ai, Jingyuan Wang

Alan G. MacDiarmid Institute of Jilin University, Changchun 130023, People's Republic of China

Received 21 August 2006; accepted 6 November 2006
DOI 10.1002/app.25809
Published online 26 April 2007 in Wiley InterScience (www.interscience.wiley.com).

ABSTRACT: The hydrophilic homopolymer brushes of poly(acrylamide) (PAAM) and poly(2-hydroxyethyl methacrylate) (PHEMA) were prepared by means of atom transfer radical polymerization (ATRP) on the modified silicon gel by the initiator that was prepared by vapor method. The block copolymer brushes consisting of PAAM and PHEMA blocks were obtained by using the homopolymer brush as the macroinitiator for the second ATRP polymerization of another monomer. The structures of the homopolymer brushes and the block copolymer brushes were characterized by IR and X-ray photoelectron spectroscopy (XPS). XPS revealed that the first polymer layer of the surface was partly covered with the second polymer layer after being block-copolymerized with the second monomer. SEM showed that the silicon gel particles with polymer brushes were made up of the silicon gel particles as the core and the polymer as the shell. Under appropriate conditions, the copper or cadmium ion was introduced into the silicon gel with the homopolymer brushes and the block copolymer brushes to form the inorganic–organic hybrid material. TGA analysis showed that the inorganic–organic hybrid material is more stable. The results of ESR indicated that the inorganic–organic hybrid material with the polymer metal complex basing on the silicon gel particle possessed well paramagnetism. J Appl Polym Sci 105: 2146–2154, 2007

Key words: ATRP; polymer brushes; polymer metal complex; inorganic–organic hybrid material; ESR

INTRODUCTION

Recently, much attention has been focused on the modification of solid surfaces,[1–7] because of their potential application in various fields of materials science such as separatory material and temperature-sensitive material. For controlling surface properties, one method that has been employed is the utilization of polymeric brushes.[8–11] Surface graft polymerization is one of the most effective and versatile methods widely used. Densely grafted molecular brushes are the most intriguing macromolecular structures and can be synthesized by ''grafting onto,'' ''grafting through,'' and ''grafting from'' methods.[12] Different from the conventional grafting, the preparation of polymer brush grafted from the surface includes two-step processes, the preparation of initiator and the controlled polymerization. Organosulfur on Au, or organosilane on silicon gel and microcontact printing, etc. have been used for the preparation of the initiator, and various polymeric reactions, including anionic, cationic, ring-opening,[13,14] radical, and metathesis polymerization,[15] have been developed to prepare the polymer brushes.

Correspondence to: J. Wang (jingyuan@jlu.edu.cn).

Journal of Applied Polymer Science, Vol. 105, 2146–2154 (2007)

Among all the polymerizations for the synthesis of polymer brushes, living polymerization is the most important one, due to its ease to control the composition of brushes. Atom transfer radical polymerization (ATRP) is one of the well-developed controlled living polymerizations.[16–21] The ATRP process involves an equilibrium reaction between a low concentration of active radicals ($R^{\bullet}$) and a much greater concentration of dormant species (RX). The equilibrium reaction is mediated via a reversible redox reaction between a transition metal complex (M_t^n/L), and the halogen-containing initiator, or dormant species (RX), forming a radical ($R^{\bullet}$) and the metal halide in a higher oxidation state (XM_t^{n+1}/L) (k_a). This radical can then initiate the polymerization of vinyl monomers (k_p). The propagating radical reacts reversibly with the metal halide to reform the lower oxidation state transition metal and an oligomer with halogen end group (k_d). In a well-controlled ATRP reaction, the concentration of radicals is held low and the contribution of the termination can often be neglected (k_t). This process can then repeat itself, resulting in the formation of the low polydispersities and predetermined molecular weight polymer (Scheme 1),[22–24] and ARTP has been proven to be effective for a wide range of monomers and appears to be a powerful tool for the polymer chemist, providing new possibilities in structural and architectural design and allowing the development of new materials with monomers currently available.

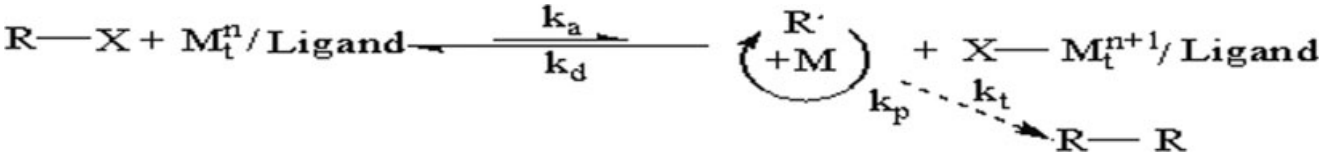

Scheme 1 The mechanism of ATRP.

Macromolecule–metal complex is a metal complex containing a polymer ligand, presenting a remarkably specific structure in which central metal ions are surrounded by an enormous polymer chain. Based on this polymeric ligand, compared with the corresponding ordinary metal complex of low molecular weight, the macromolecule–metal complex shows widely applied prospects and values in the fields of catalytic reactions, optical sensory materials, chemical sensors, magnetic materials, and those in connection with biochemistry and environmental chemistry, and to development of the novel composite materials, it has an important significance. So they have aroused some scientists' much more attention in recent years.[25,26] Currently, many researches on the polymer brushes or macromolecule–metal complex have been extensively carried out respectively, but the researches on the combination of the polymer brushes with polymer metal complex have been seldom reported. In this article, the homopolymer brushes and block copolymer brushes were prepared by combining of initiator and the ATRP technique. The initiator was prepared by vapor method. The first PHEMA brush was grafted from the surface initiator monolayer and then it was used as the macromonomer initiator to form PAAM block copolymer brush. By using the amide in AAM and the hydroxyl in HEMA complex with the metal ions to form the complexing bond, the metal ions were introduced into the polymer brushes on the silicon gel particles to synthesize the inorganic–organic hybrid material with the polymer metal complex. The resulting hybrid particles with polymer brushes and polymer metal complex were analyzed by FTIR, XPS, SEM, TGA, and ESR measurements.

EXPERIMENTAL

Materials

2-Hydroxyethyl methacrylate (HEMA) was purified by initially dissolving the monomer in water (25 vol %) containing hydroquinone (0.1 wt %). The solution was extracted 10 times with hexane to remove diacrylates and the aqueous solution was salted (200 g of NaCl/L). The monomer was then separated from the aqueous phase by diethylether extraction (four times) to remove acrylic acid. Hydroquinone (0.05 wt %) and $MgSO_4$ (3 wt %) were added to the ether solution before the ether was distilled. The purified monomer was distilled immediately prior to use.[27] Acrylamide (AAM) supplied by Shanghai Chemical Co. (A.R., 98.5%) was purified by recrystallization with acetone. Silicon gel was purchased from Qingdao Meigao Co. (10 μm, sphericity). 3-Aminopropyl triethoxysilane (99.0%) (Aldrich), Dl-ethyl-bromopropionate (99.0%) (ACROS), and 2-bromopropionyl bromide (97.0%) (Fluka) were used without further purification. CuCl purchased from Shanghai Chemical (Shanghai, China) (A.R., 97.0%) was purified by stirring in acetic acid, filtered, washed with ethanol, and dried. 2,2′-Bipyridine (bpy) (A.R., 97.0%) and triethylamine (A.R., 99.0%) were provided by Beijing Chemical Co. (Beijing, China). *N*,*N*-dimethylformamide (DMF) was freshly distilled before use. Toluene purchased from Beijing Chemical (A.R., 99.0%) was dried by calcium hydride for 24 h and distilled. $CuCl_2{\cdot}2H_2O$ (A.R.) and $CdCl_2{\cdot}2.5H_2O$ (A.R.) were purchased from Beijing Chemical and used without further purification.

Characterization

The Fourier transform infrared (FTIR) spectra of the polymer brushes on silicon gel were carried out using a Nicolet FT/IR-410. The X-ray photoelectron spectra (XPS) measurements were carried out with an Escalab mark II apparatus. Thermogravimetric analysis (TGA) was recorded on a Pyris Diamond Tg-DTA (Perkin-Elmer Thermal Analysis). The morphologies of the polymer brushes were observed with a SEM (SHIMADZU SSX-550). The electron spin resonance (ESR) of metal complexes was investigated by means of Bruker (Germany) ESR ER200D-SRC.

Preparation of initiator

The synthesis of initiator was carried out according to Scheme 2. Twenty milliliters of HCl, 87 mL of H_2O, and 2.0 g of silicon gel were mixed, and the mixture was stirred under refluxing for 11 h. The silicon gel was washed with a large amount of water to remove the absorbed HCl. Thirty milliliters of toluene, 5 mL of KH-550, and 2.0 g of activated silicon gel were mixed and the mixture was stirred under refluxing for 10 h. The silicon gel was washed with toluene and acetone and dried under vacuum at 40°C for 24 h. Then 10 mL of toluene, 2.4 mL of 2-bromopropionyl bromide, and

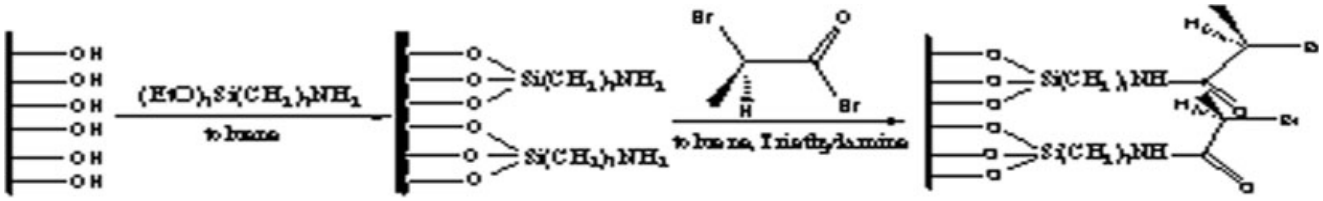

Scheme 2 The synthetic route of initiator on silicon gel.

2 mL of triethylamine were mixed with the modified silicon gel and the mixture was stirred at room temperature for 3 h. The silicon gel was washed with toluene and acetone and dried under vacuum.

Preparation of PAAM polymer brush on silicon gel

A dry round bottom flask was charged with 0.01 g of CuCl, 0.047 g of bpy, 2.5 g of AAM, and 0.2 g of initiator of silicon gel. The flask was sealed with a rubber septum and was cyclically treated under vacuum and argon three times to remove the oxygen. Then a solution of DMF and DL-ethyl-bromopropionate (1 μL) was added to it with a syringe. The flask was immersed in a 110°C oil bath. After several hours, the polymerization solution was cooled to room temperature to terminate the polymerization. The polymer solution was diluted with DMF and silicon gel was precipitated. The silicon gel was washed with H_2O and acetone to remove the adsorbed free PAAM.

Preparation of PHEMA polymer brush on silicon gel

The polymerization of HEMA was carried out under the same polymerization conditions as shown above except the temperature (100°C).

Preparation of PAAM/PHEMA (PHEMA/PAAM) block polymer brushes on silicon gel

After the first layer of PAAM (or PHEMA) brush formed, the polymer brush was used as the anchored-initiator for the polymerization of HEMA (or AAM) using the same polymerization condition as shown above.

Preparation of metal complexes

The silicon gel with PAAM polymer brush was dispersed in H_2O and a aqueous solution of $CuCl_2{\cdot}2H_2O$ was added; then, the solution was stirred at 80°C for 24 h, and the silicon gel was washed with H_2O several times to remove the absorbed Cu^{2+}. Then, the silicon gel was dried at room temperature under vacuum and a green powder was obtained. The procedure of preparing the PAAM-Cd^{2+} metal complex is almost the same as that of preparing PAAM-Cu^{2+}. The difference is that the aqueous solution of $CdCl_2{\cdot}2.5H_2O$ was added into the silicon gel with PAAM solution and then a yellow powder was formed. The silicon gel with PHEMA polymer brush was dispersed in DMF and H_2O, a $CuCl_2{\cdot}2H_2O$ ($CdCl_2{\cdot}2.5H_2O$) ammonia solution was added and the solution was stirred at 70°C for 24 h, and the silicon gel was washed with H_2O several times to remove the absorbed Cu^{2+} (Cd^{2+}). Then, the silicon gel was dried at room temperature under vacuum and a green (yellow) powder was obtained. The silicon gel with PAAM/PHEMA (PHEMA/PAAM) block polymer brush was dispersed in H_2O and DMF; the other complex conditions are almost the same as those of preparing PHEMA-Cu^{2+}.

RESULTS AND DISCUSSION

Characterization of polymer brushes

To prepare the polymer brush from surface, a uniform and densely packed initiator-modified substrate is indispensable. The initiator was prepared by vapor method. The silicon gel was treated with the vapor of 3-aminopropyl triethoxysilane, followed by amidization with 2-bromopropionyl bromide. After surface modification, XPS was used to confirm the formation of the initiator monolayer. The peak of Br 3d (the content of Br: 6%) was observed around the binding energy (BE) at 71 eV on the silicon gel surface treated indicating the formation of the monolayer (Fig. 1).[28] Besides the Br 3d peak, another two peaks of Si 2p were found at 104.3 and 101.6 eV, which were assigned to the Si—O—Si and C—Si—O, respectively, which are unambiguous proof of the presence of a grafted organic layer on the surface of the hybrid inorganic/organic particles. All these data show that the silicon gel has been modified.

To obtain a hydrophilic polymer brush, the polymer should be accumulated successively by controlled living polymerization. ATRP has been successfully used in the polymerization to yield narrow polydispersity homopolymers.[29] The PAAM brush was reported by Huang and Wirth.[30] The main challenge in ATRP carried out on surfaces with very low concentrations of initiating groups stems from the fact that, after the halogen atom transfers to the transition metal catalyst, the concentration of persistent radical may be too low

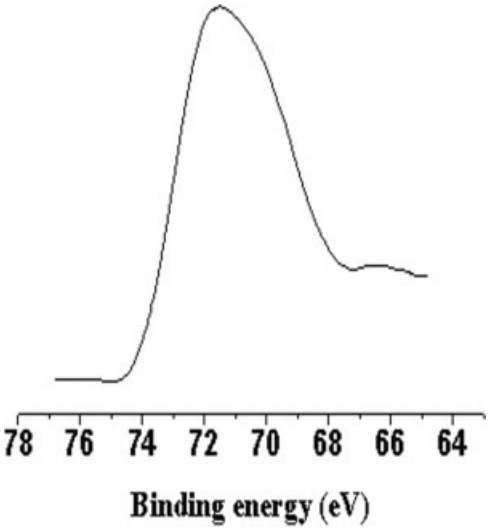

Figure 1 XPS spectra of the initiator modified with self-assemble: the peak of Br 3d.

to reversibly trap the propagating radicals, leading to uncontrolled chain growth. This challenge can be effectively addressed through the addition of a ''sacrificial initiator,'' at the beginning of the reaction. The free initiator plays not only as an indicator of the polymerization but also as a controller for the ATRP on the surface. In this work, we chose AAM and HEMA as two monomers for the preparation of block copolymer brushes and DL-ethyl-bromopropionate as a ''sacrificial initiator.'' Because we attempted to characterize the polymer by surface-initiated polymerization, we

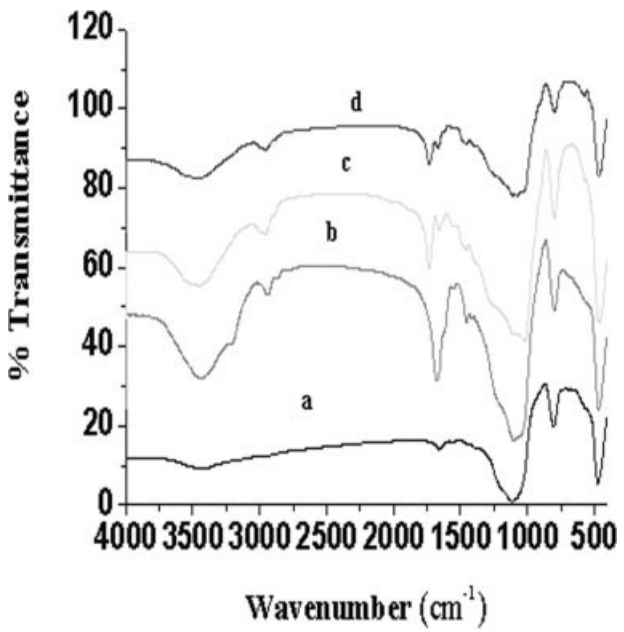

Figure 2 FTIR spectra of (a) initiator, (b) PAAM, (c) PHEMA, and (d) PAAM/PHEMA brushes on the silicon gel.

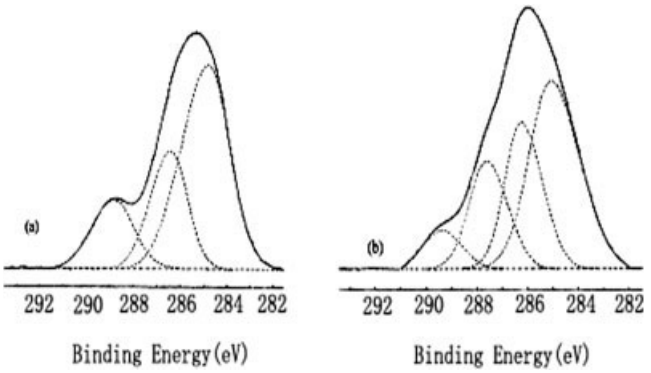

Figure 3 C 1s XPS spectra of (a) PAAM and (b) PHEMA homopolymer brushes on the silicon gel.

detached the grafted polymer films from their substrates. Unfortunately, the detached polymer was insoluble. The most reasonable explanation for this is intermolecular crosslinking via transesterification.[31] Therefore, we cannot obtain the molecular weight of the polymer brush to monitor the surface-grafted polymerization process.

Figure 2 shows the IR spectra of the polymer brushes on the silicon gel. In the spectrum of PAAM brush, a broad absorption peak can be seen in the region of 3200–3500 cm^{-1} (N—H stretching vibration in amide), and two absorption peaks appeared at 1665 and 1615 cm^{-1} (carbonyl in amide due to the formation of hydrogen bond with amide group).[32] It indicates that PAAM brush has grown from the silicon gel surface. In the spectrum of PHEMA brush, a sharp absorption peak appears at 1735 cm^{-1} (carbonyl stretching vibration in ester) and it indicates that PHEMA brush has grown from the surface of silicon gel. In the case of the block polymer brush of Si/PHEMA/PAAM (Si/PAAM/PHEMA), the absorption peaks of carbonyl stretching vibration in ester and in amide were observed, respectively. It shows that after the formation of homo-grafting polymerization of PHEMA brush, as the macroinitiator for the second polymerization, which is active, the block polymerization from the first polymer brush was carried out. On the other hand, as the intensity of carbonyl absorption peak in ester or acrylamide is very strong compared

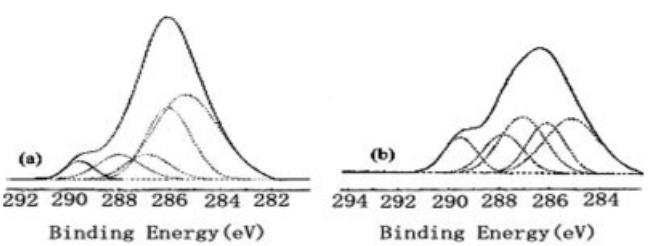

Figure 4 C 1s XPS spectra of (a) PHEMA/PAAM and (b) PAAM/PHEMA block polymer brushes on silicon gel.

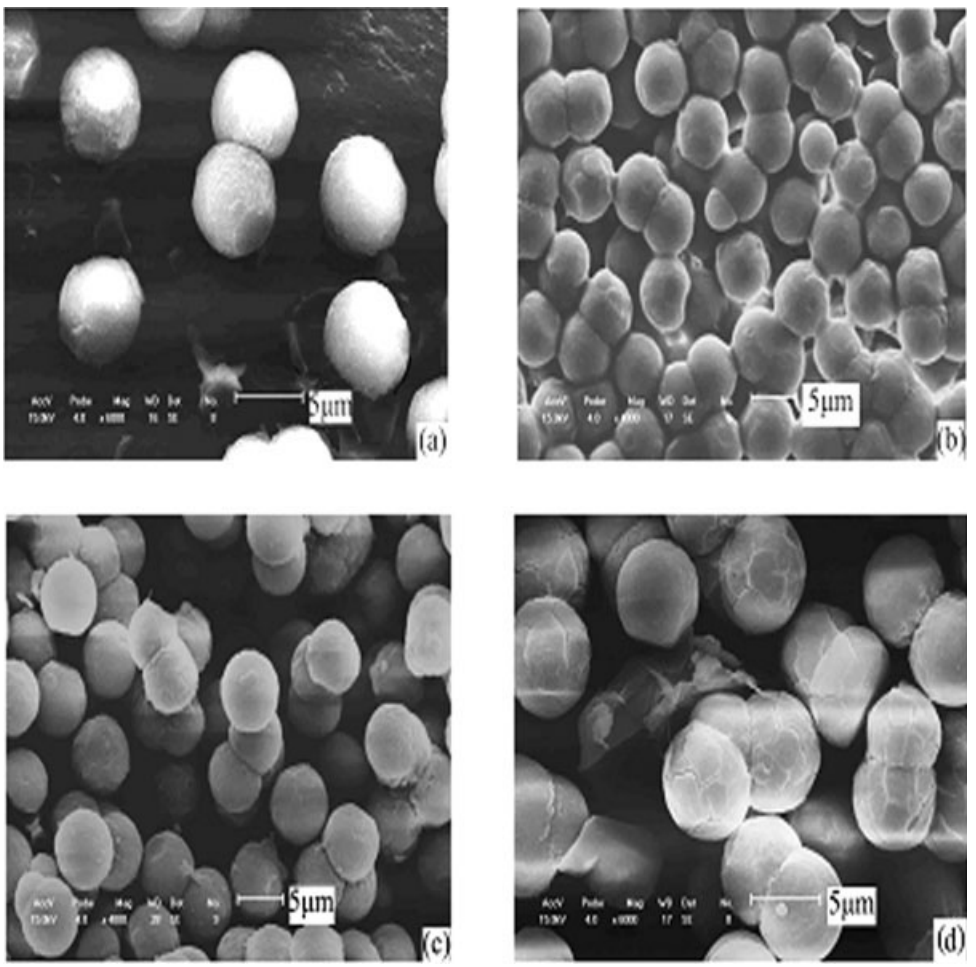

Figure 5 SEM images of (a) silicon gel particle, (b) PAAM polymer brush on the silicon gel, (c) PHEMA polymer brush on the silicon gel, and (d) PAAM/PHEMA polymer brush on the silicon gel.

with Si—O absorption peak (1090 cm^{-1}), the polymer layers of the HEMA and AAM grafted from silicon gel are thick.

XPS analysis were carried out to determine the surface compositions of the uncoated and polymer-grafted silicon gel. In these experiments, the Si 2p signal acts a marker for the silicon gel and almost all of the C 1s signal is due to the surface-grafted polymer chains (a small fraction is also due to the initiator) and N can be used as unambiguous elemental markers for the grafted polymer component for AAM monomer. Both the Si/PAAM and the Si/PHEMA/PAAM block polymer brushes showed the N 1s peak, indicating the formation of PAAM brush on the substrate. In the XPS spectra of the PAAM and PHEMA homopolymers and their block polymers, all the C 1s peaks appeared around 285 eV with a broad shoulder at the higher binding energy. According to the Ref. 33, careful peak fitting on the C 1s peaks resolves three peaks representing different carbons in PAAM: (1) aliphatic hydrocarbon (*C*—C at 284.8 eV), (2) an amide induced, β-shifted carbon (*C*—$CONH_2$ at 286.3 eV), and (3) the amide carbon ($CONH_2$ at 288.6 eV) [Fig. 3(a)]. Similarly, the PHEMA showed four kinds of carbon: (1) aliphatic hydrocarbon (*C*—C/*C*H, at a binding energy of 284.9 eV), (2) an ester-induced, β-shifted carbon (*C*—COO at 286.1 eV), (3) the methylside ester (*C*—O at 287.5 eV), and (4) the carboxyl carbon(*C*=O at 289.4 eV) [Fig. 3(b)]. On the basis of the above results, the C 1s peaks of the block polymers were fitted. Figure 4 shows the peak-fitting curves of the C 1s peaks of block polymer brushes. The ratio of C 1s peak area of carbonyl of PHEMA (ester at 289.5 eV) to that of PAAM (amide at 288.1 eV) in the Si/PHEMA/PAAM brush was found to be 1 : 2 [Fig. 4(a)] and the ratio of C 1s peak area of carbonyl of PAAM (amide at 287.9 eV) to that of PHEMA (ester at 289.6 eV) in the Si/PAAM/PHEMA brush was found to be 13 : 10 [Fig. 4(b)], indicating that the surface should contain two kinds of blocks, PHEMA and PAAM. Therefore, the surface was not completely covered by the second layer of polymer. This result is consistent with the IR results.

Figure 5 depicts the scanning electron micrographs of the silicon gel before and after the surface-initiated polymerization. In Figure 5(a), the silicon gel particle

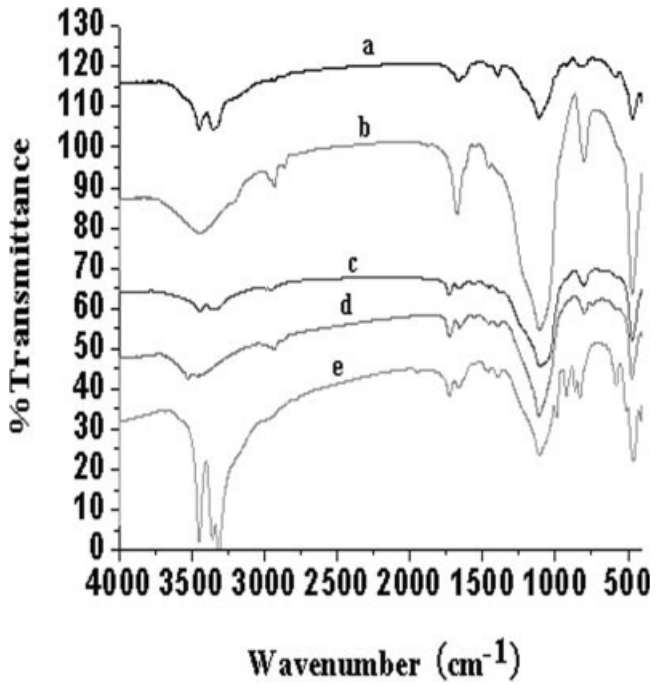

Figure 6 FTIR spectra of (a) PAAM-Cu^{2+}, (b) PAAM-Cd^{2+}, (c) PHEMA-Cu^{2+}, (d) PHEMA-Cd^{2+}, and (e) PAAM/PHEMA-Cu^{2+} on the silicon gel.

morphology is confirmed to be monodisperse sphere with smooth surface as expected. The diameter of particle is about 5 μm. In Figures 5(b) and 5(c), the diameter of particles with PAAM (PHEMA) polymer brush is about 7 μm, the surface of these silicon gel particles become rough obviously, which suggests that silicon gel particle is coated by a relatively thick layer of PAAM (PHEMA) chains. We also noticed that the hybrid particles were composed of the organic shell and the inorganic core. Furthermore, the aggregate particles appeared because the chains of high content polymers on the surface of spherical silicon gel particles were twisted each other. Figure 5(d) shows the morphology of the particle with PAAM/PHEMA polymer brush. In Figure 5(d), the surface of the silicon gel particle is rougher due to the high content of organic shell. Furthermore, the silicon gel particles with polymer brush are very equirotal, which indicates that the content of polymer can be controlled by ATRP and the organic content of the surface of per silicon gel particle is almost equal.

Characterization of metal hybrids

Figure 6 shows the IR spectra of the polymer metal complexes on the silicon gel particles. Compared with the spectrum of PAAM brush on the silicon gel [Fig. 2(b)], in the spectrum of PAAM metal (Cu^{2+}) complex on the silicon gel, a new broad absorption peak was observed in the region of 3320–3360 cm^{-1} and the absorption peak appeared at 1685 cm^{-1} was shifted to 1665 cm^{-1} due to introducing the metal (Cu^{2+}). Similarly, in the spectrum of PHEMA metal (Cu^{2+}) complex on the silicon gel, a new broad absorption peak was also observed in the region of 3320-3360 cm^{-1}, because the metal (Cu^{2+}) complex possessed —OH and in the spectrum of PAAM/PHEMA metal (Cu^{2+}) complex on the silicon gel, two absorption peaks appeared at 3320 and 3360 cm^{-1} because metal (Cu^{2+}) complexes with —NH_2 and —OH, respectively. These indicate that the inorganic–organic hybrid material with the polymer metal (Cu^{2+}) complex has been synthesized, but the obvious change was not detected in the spectrum of polymer metal (Cd^{2+}) complex.

Figure 7 shows the XPS of the polymer metal complex. Figure 7(a) shows the XPS spectra of Cu 2p of the PAAM-Cu^{2+} complex on the silicon gel. This is the typical XPS of Cu^{2+} and it indicates that the state of Cu^{2+} is not changed. According to the expressions:

$$C_x = (A_x/S_x)/\left(\sum A_i/S_i\right)$$

where A is the peak area of different element and S is the sensitive factor. The content of Cu^{2+} on the surface of the silicon gel is 2.0%. It is larger than the content of Cd^{2+} (0.16%) of PAAM-Cd^{2+} complex on the silicon gel. These show that the strength of M—N bond in the row of metal ions decreased in the order: $Cu^{2+} > Cd^{2+}$. The rows of steadiness of the crosslinked mac-

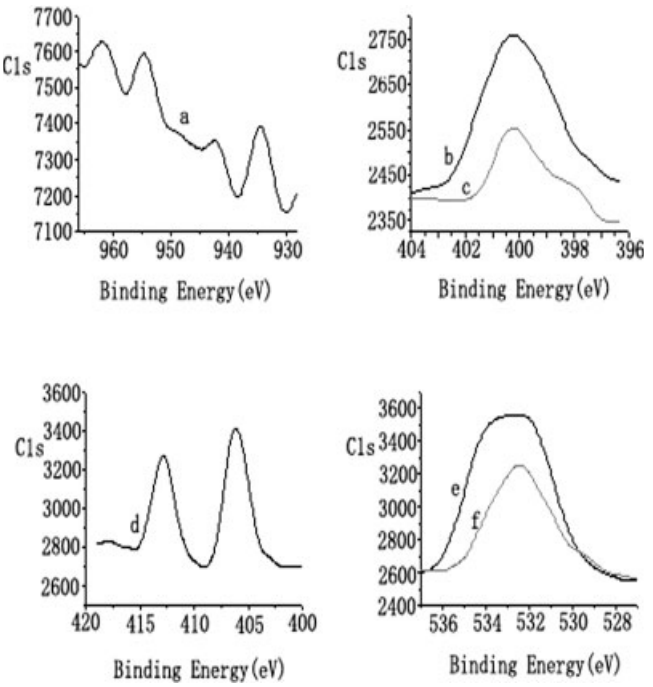

Figure 7 XPS spectra of (a) Cu^{2+} 2p of PAAM-Cu^{2+}, (b) N 1s of PAAM brush, (c) N 1s of PAAM-Cu^{2+}, (d) Cd^{2+} 3d of PHEMA-Cd^{2+}, (e) O 1s of PHEMA brush, and (f) O 1s of PHEMA-Cd^{2+} on the silicon gel.

TABLE I
TGA and Metal Content of Polymer and Polymer Metal Complex

Sample	TGA (%)[a]	Decompose temperature (°C)	Cu (%)[b]	Cd (%)[b]	Cu $2p_{3/2}$ binding energy (eV)	Cd $2p_{3/2}$ binding energy (eV)
PAAM	37.0	215.6				
PHEMA	42.8	262.6				
PAAM-*b*-PHEMA	44.7	210.5				
PAAM-Cu^{2+}	32.8	235.9	2.0		934.2	
PHEMA-Cd^{2+}	38.2	289.7		4.8		406
PAAM-*b*-PHEMA-Cu^{2+}	34.5	248.3	6.0		934.5	

[a] Heating from 20.00°C to 800.00°C at 10.00°C/min.
[b] Measured by X-ray photoelectron spectroscopy.

rocomplexes of this type are usually in the coincident with famous Williams–Irving stability row for low molecular ligands. Figure 7(b,c) shows the XPS spectra of N 1s of PAAM brush on the silicon gel and PAAM-Cu^{2+} complex on the silicon gel, respectively. These testify that PAAM brush has grown from the silicon gel surface. Compared with Figures 7(b) and 7(c), we find the obvious change, and the content of N in Figure 7(c) is less than that in Figure 7(b). These indicate that the metal ions have already been introduced into the hybrid material system. Figure 7(d) shows the XPS spectra of Cd 3d of PHEMA-Cd^{2+} complex on the silicon gel. The value of the binding energy is Cd $3d_{3/2} = 406.00$ eV, compared with the value in the Handbook of X-ray Photoelectron Spectroscopy, the Cd^{2+} existed as $CdCl_2$. The content of

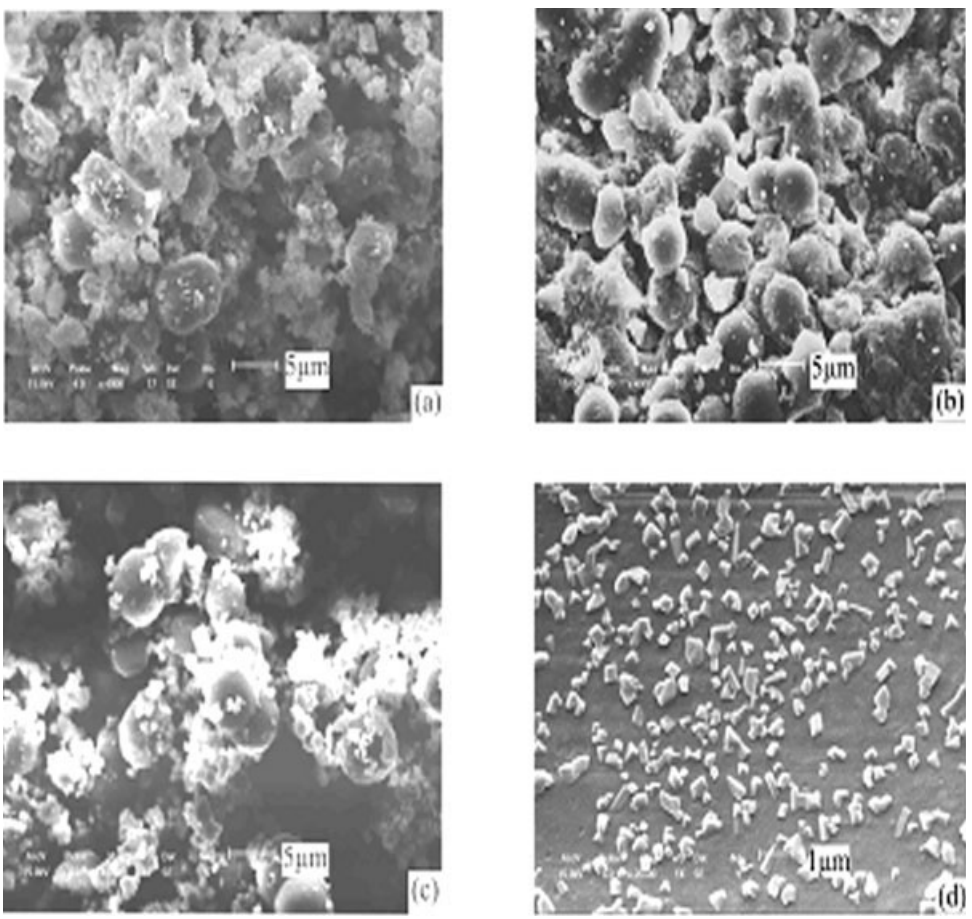

Figure 8 SEM images of (a) PAAM-Cu^{2+} on the silicon gel, (b) PHEMA-Cd^{2+} on the silicon gel, (c) PHEMA/PAAM-Cu^{2+} on the silicon gel, and (d) PAAM-Cu^{2+} on the silicon gel after being eroded in solution of HF.

Cd^{2+} of PHEMA-Cd^{2+} complex on the surface of the silicon gel is 4.8% via calculation and is larger than that of Cu^{2+} (2.2%) of PHEMA-Cu^{2+} complex on the silicon gel. This shows that the strength of M—O bond is $Cd^{2+} > Cu^{2+}$. Figure 7(e,f) shows the XPS spectra of O 1s of PHEMA brush on the silicon gel and PHEMA-Cd^{2+} complex on the silicon gel, respectively. In Figure 7(f), the binding energy peak of Cd—O bond was obviously observed. Similarly, the same conclusions are deduced from the XPS spectra of the PAAM-*b*-PHEMA metal (Cu^{2+}) complex on the silicon gel and PHEMA-*b*-PAAM metal (Cu^{2+}) complex on the silicon gel as shown above. In Table I, the values of binding energy and the contents of metal ions are listed in detail. From the data, we can find that the contents of the metal ions in the PAAM metal complexes are generally lower than those in the PHEMA metal complexes, which means that the hydroxyl in HEMA is stronger than the amide in AAM for complexing the metal ions, and the content of the metal ion in PHEMA-*b*-PAAM metal (Cu^{2+}) complex is larger than those in the others, which indicates that the block copolymer has been synthesized and the ability of the silicon gel particle complexes with the metal ions got stronger. This result is consistent with the IR results.

Figure 8 shows the morphologies of PAAM metal (Cu^{2+}) complex on the silicon gel, PHEMA metal (Cd^{2+}) complex on the silicon gel, PHEMA/PAAM metal (Cu^{2+}) complex on the silicon gel, and PAAM metal (Cu^{2+}) complex on the silicon gel after it was eroded in a solution of HF. Compared with Figure 5(b–d), we can see that for the polymer metal complex, uniform spherical particles were not formed, indicating that the metal ions greatly affect the morphologies of the silicon gel particle with polymer brush. In this system, metal ion is a center and the polymer is a ligand. The center metal ion complexes with several N atoms in PAAM or O atoms in PHEMA, which shows that the metal ions resemble the crosslink agent, resulting in the formation of a network structure with polymer. The two forms are manifested to be crosslink. On the one hand, the polymer chain wraps on the surface of per silicon gel particle, and on the other hand, several silicon gel particles have interaction. These indicate that the morphologies of the single silicon gel particle and the whole silicon gel particles have been changed obviously. Figure 8(d) shows the morphologies of the PAAM metal (Cu^{2+}) complex on the silicon gel after it was eroded in a solution of HF. On the surface of PAAM film, the metal ions with about 250 nm in size were uniformily distributed. These further prove that the metal ions have been introduced into the silicon gel particle with polymer brush and the polymer metal complexes on the silicon gel particle were prepared.

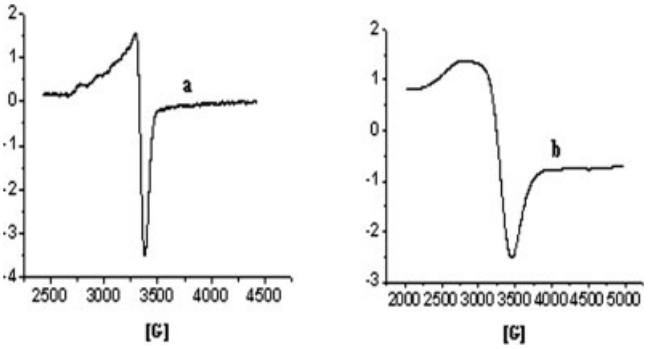

Figure 9 ESR spectra of (a) PAAM-Cu^{2+} and (b) PAAM/PHEMA-Cu^{2+} on the silicon gel.

To provide the information of the grafting density and thermal stability of polymer brush on the silicon gel and polymer metal complex on the silicon gel, TGA was used. Indeed, the TGA allow us to decompose all the organic residues (initiator and polymer) and thus recover the inorganic part, i.e., pure silicon gel particle and metal ions, the final weight corresponding to the silicon gel particle and metal ions, and the weight loss to the grafted polymers. In Table I, TGA and decomposition temperature of polymer brush on the silicon gel and polymer metal complex on the silicon gel are given. From these data, we can find that the decomposition temperature of the polymer brushes on the silicon gel is lower and the TGA values of polymer brushes are higher compared with those of the polymer metal complexes. This is due to introducing the metal ions into the polymer brushes on the silicon gel particle and the amide in AAM and the hydroxyl in HEMA complex with the metal ions forming the complexing bond, which led to the formation of space network structure of the polymer brush and the increasing of the crosslinking degree of the polymer brush. This was observed in Figure 8. The stability of the polymer brushes was increased because of these factors.

The ESR technique is an important method which to characterization for MMC containing paramagnetic ions. The information provided by ESR may give a detailed description of metal ion valence state, the nature of ligands and bonds, and orientation of bound complexes.[34] Figure 9 is the ESR spectra of PAAM metal (Cu^{2+}) complex on the silicon gel particle and PAAM/PHEMA metal (Cu^{2+}) complex on the silicon gel particle. Figure 9(a) shows that the Cu^{2+} complex is well paramagnetic and according to the expressions, $g = hv/(\beta Hr)$, we know the g values ($g_{//} = 2.3331$, $g_{\perp} = 2.0831$). Because $2.02 < g_{\perp} < g_{//}$, the ESR spectrum is axial symmetry, the Cu^{2+} ions are anisotropic, the uncoupled electron lies in the orbit of $d_{x^2} - y^2$, namely, ligand field ground stated is $^2B_{1g}$, furthermore, the circumstance central metallic ions are different,[35,36] and the curve is multithreading and the superfine appears,

which indicates that Cu^{2+} ions of PAAM metal complex on the silicon gel particle have almost no interaction. In Figure 9(b), the curve is broad and the superfine structure does not appear, which elucidates that the material is combo and the particle displays intense reciprocity with each other. From Figure 9, we know that with increasing Cu^{2+} content, the form of complexes vary from isolated centers to aggregates, the reaction of metal ions of polymer metal complex on the silicon gel particle has almost no interaction vary to strong spin–exchange interaction, ESR spectra vary from multiplet to singlet. All the ESR data demonstrate that the novel inorganic–organic hybrid material with the polymer metal complex exhibits excellent paramagnetic property.

CONCLUSIONS

In this article, on the basis of self-assembly method to modify the silicon gel on which the grafted organic compound including the halogen was used as the initiator of ATRP, homopolymers and block hydrophilic polymer brushes were prepared by means of ''graft from'' method. Because the spherical silicon gel is still retainable after modified by a polymer, the polymer can be entitled ''spherical polymer brush.'' On the other hand, the particles of the hybrid materials are equirotal, which indicates that the content of polymer can be controlled by ATRP. The formation of PHEMA and PAAM polymer brushes was confirmed by FTIR spectra and XPS spectra. The compositions of the block polymer brushes were investigated by XPS. The PHEMA block in the Si/PHEMA/PAAM brush covers 33% of the surface, and the AAM block in the Si/PAAM/PHEMA brush covers 57% of the surface. These hybrid particles from the functional monomer (AAM or HEMA) via ATRP can form the polymer metal complex on the surface of silicon gel by introducing metal ions (Cu^{2+} and Cd^{2+}). The results of TGA show that owing to the introduction of the metal ions into the hybrid particles, the amide in AAM and the hydroxyl in HEMA complex with the metal ions formed the complexing bond, the stability of the particles was increased, and the data of ESR indicate that the inorganic–organic hybrid particles of the polymer metal complex based on silicon gel possess paramagnetism. We synthesized the hybrid materials of polymer metal complexes that possess the properties of inorganic silicon gel, polymer, and metal ions. This kind of novel functional hybrid materials may be used as magnetic material, catalyzer, analysis and separatory material.

References

1. Prucker, O.; Ruehe, J. Macromolecules 1998, 31, 602.
2. Werne, T. V.; Patten, T. E. J Am Chem Soc 2001, 123, 7497.
3. Nuss, S.; Bottcher, H.; Wurm, H.; Hallensleben, M. L. Angew Chem Int Ed 2001, 40, 4016.
4. Vestal, C. R.; Zhang, Z. J. J Am Chem Soc 2002, 124, 14312.
5. Khan, M.; Huck, W. T. S. Macromolecules 2003, 36, 5088.
6. Kong, H.; Gao, C.; Yan, D. Y. J Mater Chem 2004, 14, 1401.
7. Xu, F. J; Xu, D.; Kang, E. T.; Neoh, K. G. J Mater Chem 2004, 14, 2674.
8. Zhao, B.; Brittain, W. J. Prog Polym Sci 2000, 25, 677.
9. Jayachandran, K. N.; Takacs-Cox, A.; Brooks, D. E. Macromolecules 2002, 35, 4247.
10. Bontempo, D.; Tirelli, N.; Masci, G.; Crescenzi, V.; Hubbell, J. A. Macromol Rapid Commun 2002, 23, 417.
11. Balamurugan, S.; Mendez, S.; Balamurugan, S. S.; O'Brien, M. J.; Lopez, G. P. Langmuir 2003, 19, 2545.
12. Schappacher, M.; Deffieux, A. Macromolecules 2000, 33, 7371.
13. Jordan, R.; Ulman, A.; Kang, J. F.; Rafailovich, M. H.; Sokolov, J. J Am Chem Soc 1999, 121, 1016.
14. Jordan, R.; Ulman, A. J Am Chem Soc 1998, 120, 243.
15. Weck, M.; Jackiw, J. J.; Rossi, R. R.; Weiss, P. S.; Grubbs, R. H. J Am Chem Soc 1999, 121, 4088.
16. Kato, M.; Kamigaito, M.; Sawamoto, M.; Higashimura, T. Macromolecules 1995, 28, 1721.
17. Wang, J. S.; Matyjaszewski, K. J Am Chem Soc 1995, 117, 5614.
18. Wang, J. S.; Matyjaszewski, K. Macromolecules 1995, 28, 7901.
19. Jones, D. M.; Brown, A. A.; Huck, W. T. S. Langmuir 2002, 18, 1265.
20. Save, M.; Weaver, J. V. M.; Armes, S. P. Macromolecules 2002, 35, 1152.
21. Robinson, K. L.; Khan, M. A.; Wang, X. S.; Armes, S. P. Macromolecules 2001, 34, 3155.
22. Patten, T. E.; Matyjaszewski, K. Adv Mater 1998, 10, 901.
23. Patten, T. E.; Matyjaszewski, K. Acc Chem Res 1999, 32, 895.
24. Matyjaszewski, K. Chem Eur J 1999, 5, 3095.
25. Oriol, L.; Serrano, J. L. Adv Mater 1995, 7, 348.
26. Zhang, H.; Ma, H.; Li, H.; Wang, J. Polym Int 2002, 51, 1129.
27. Beer, K. L.; Boo, S.; Gaynor, S. G.; Matyjaszewski, K. Macromolecules 1999, 35, 5772.
28. Grimaud, T.; Matyjaszewski, K. Macromolecules 1997, 30, 2216.
29. Rieke, P. C.; Baer, D. R.; Fryxell, G. E.; Engelhard, M. H.; Porter, M. S. J Vac Sci Technol A 1993, 11, 2292.
30. Huang, X.; Wirth, M. J. Macromolecules 1999, 32, 1694.
31. Huang, W. X.; Kim, J. B.; Bruening, M. L.; Baker, G. L. Macromolecules 2002, 35, 1175.
32. Silverstein, R. M.; Webster, F. X. Spectrometric Identification of Organic Compounds, 6th ed.; Wiley: New York, 1997.
33. Watts, J. F.; Leadley, S. R.; Castle, J. E.; Blomfield, C. J. Langmuir 2000, 16, 2292.
34. Ciardelli, F.; Tsuchida, E. T.; Wohrle, D., Eds. Macromolecule-Metal Complex; Springer: Berlin 1996; p 43.
35. Hathaway, B. J.; Billing, D. E. Coord Chem Rev 1970, 6, 143.
36. Molochnikov, L. S.; Kovalyova, E. G.; Zagorodni, A. A.; Muhammed, M.; Sultanov, Y. M.; Efendiev, A. A. Polymer 2003, 44, 4805.